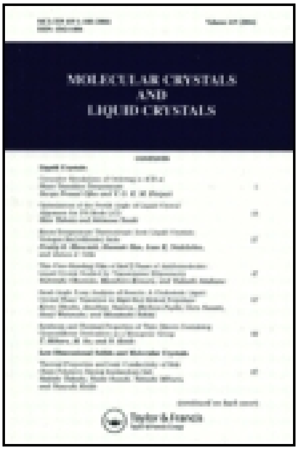

Molecular Crystals and Liquid Crystals
Publication details, including instructions for authors and subscription information:
http://www.tandfonline.com/loi/gmcl20

A New Insight on the Bistability and Relevant Phenomena in Ferroelectric Smectic C* Liquid Crystals

L. M. Blinov [a] & S. P. Palto [b]

[a] INFM, Dipartimento di Fisica, Università della Calabria, Arcavacata di Rende (Cs), Italy and Institute of Crystallography, Russian Academy of Sciences, Leninsky, Moscow, Russia

[b] Institute of Crystallography, Russian Academy of Sciences, Leninsky, Moscow, Russia

Version of record first published: 31 Aug 2006

To cite this article: L. M. Blinov & S. P. Palto (2005): A New Insight on the Bistability and Relevant Phenomena in Ferroelectric Smectic C* Liquid Crystals, Molecular Crystals and Liquid Crystals, 429:1, 31-53

To link to this article: http://dx.doi.org/10.1080/15421400590930656

Mol. Cryst. Liq. Cryst., Vol. 429, pp. 31–53, 2005

ISSN: 1542-1406 print/1563-5287 online
DOI: 10.1080/15421400590930656

A New Insight on the Bistability and Relevant Phenomena in Ferroelectric Smectic C* Liquid Crystals

L. M. Blinov
INFM, Dipartimento di Fisica, Università della Calabria,
Arcavacata di Rende (Cs), Italy and Institute of Crystallography,
Russian Academy of Sciences, Leninsky, Moscow, Russia

S. P. Palto
Institute of Crystallography, Russian Academy of Sciences,
Leninsky, Moscow, Russia

The physics of the bistability and relevant phenomena in smectic C liquid crystals has been discussed. The problem is treated in terms of the director and not of its projection onto the smectic plane (the so-called c-director). As in the case of nematic liquid crystals, two anchoring energies are considered to be important, the zenithal and the azimuthal ones, both are unpolar. This allows the derivation of a new, basic criterion for the bistability of the director switching in the ferroelectric cells without alignment layers or with strongly conductive alignment layers. In the case of weakly conductive alignment layers, an additional criterion has been found that originates from the internal field in a liquid crystal cell opposite to the external field. This field can cause monostable director switching or an inverse bistability. It is also responsible for the hysteresis-free switching and the electrooptical V-shape effect in the smectic C* phase.*

Keywords: bistability; ferroelectricity; liquid crystals; simulation; V-shape effect

1. INTRODUCTION

Ferroelectric liquid crystals (FLC) having a chiral smectic C^* structure [1], possess an intrinsic polarity and can be driven to the "on" and "off" states by an external a.c. voltage. In a confined geometry, when an

Authors are grateful to M. I. Barnik, A. R. Geivandov, S. A. Pikin, E. P. Pozhidaev for many discussions and acknowledge the financial support from Russian Foundation for Basic Research (grants no.03-02-17288 and 04-02-16466). S. P. Palto has also been supported by Russian Science Support Foundation.
Address correspondence to L. M. Blinov, E-mail: blinov@fis.unical.it

FLC structure is stabilised by surfaces, the two ferroelectric states have intrinsic memory, and the electrooptical switching of the FLC manifests a threshold behaviour with a characteristic hysteresis [2,3]. This, so-called Clark-Lagerwall effect has many common features with the well known bistability phenomenon in solid ferroelectrics. The lifetime of the two stable states is a key issue for the application of FLCs to the display technology. The experiments show that many factors influence the bistability. The physics of the bistability phenomenon in FLC cells is not well understood yet. It is evident that the aligning layers play the crucial role because, first of all, they determine the strength of the FLC anchoring and, second, they provide the internal field in the FLC layers that very often eliminates the bistability [4].

Recently three groups from the Institute of Crystallography, Lebedev Physical Institute (both from Russian Academy of Sciences) and Darmstadt Technical University have carried out extensive experimental works and computer simulations focused onto the physics and applications of the bistability, hysteresis-free switching and V-shape effect in FLCs [5–9]. For interpretation of the experimental results a new software has been developed which has taken into account all basic properties of the smectic C* phase and aligning layers relevant to the problem of bistability [10]. For the first time the problem has been treated in terms of the director itself and not of its projection onto the smectic plane (the so-called c-director or azimuthal angle φ). The results of modelling show that, as in the case of nematic liquid crystals, two anchoring energies are of paramount importance, the zenithal and the azimuthal ones, *both are unpolar*. This allows the derivation of a new, basic criterion for the bistability of the director switching in the ferroelectric cells without alignment layers or with the layers of infinite conductivity [9]. We believe that the *polar* anchoring energy may be neglected, at least, when interpreting experiments with modern FLC materials and cell constructions. We also disregard flow effects and any domain structures because the main features of the phenomena discussed may be understood without these complications. In the case of weakly conductive alignment layers, an additional criterion has been found that originates from an internal field in the cell. After the end of the external voltage pulse, this field of the opposite sign still exists for a certain time and is responsible for the final state of the director. We can show how this field causes the monostable director switching observed in [11] or even the inverse bistability observed in FLC drops dispersed in a polymer [12]. It is also responsible for the hysteresis-free switching and the electrooptical V-shape effect in the smectic C* phase [7,8].

This paper is an extended version of the invited talk made by L. Blinov on behalf of both the co-authors at the Meeting of the Italian Liquid Crystal Society in June, 2004 (SICL-04). To some extent the paper keeps the style of the oral presentation. It is devoted to the physical aspects of the bistability and also reflects our point of view on some relevant topics including the very existence of ferroelectricity in the SmC* phase. This concept is discussed in the beginning of the paper. Then we consider the problem of the director anchoring in the SmC* phase and discuss the threshold for the director switching. When it is possible we make comparison of the SmC* phase with the nematic one. Further on, we consider the bistability criteria for "ideal" FLC cells with electrodes playing an additional role of alignment layers. In this case, the FLC feels only the external field. Then the role of the internal field existing in real cells is analysed and our modelling results are shown.

2. "FERROELECTRICITY" IN THE SmC* PHASE

The structure of the non-chiral smectic C phase is shown in Figure 1. It belongs to the D_2^h point group symmetry and is described by the

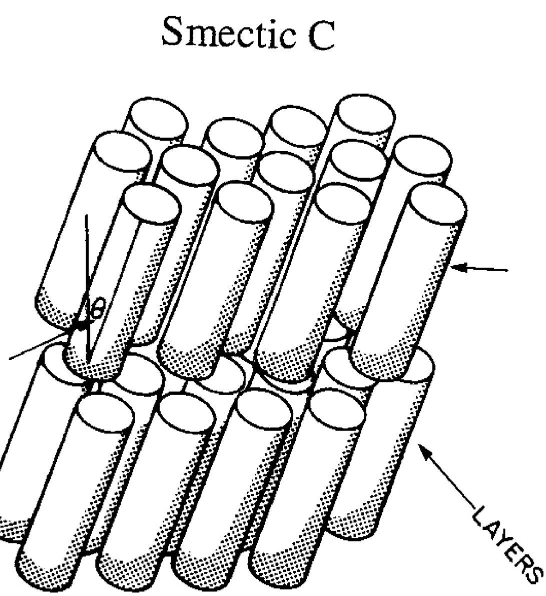

FIGURE 1 Structure of the non-chiral SmC phase.

two-component order parameter

$$\eta = \vartheta \exp \mathrm{i}\varphi \qquad (1)$$

associated with the smectic A–C transition. In Eq. (1) ϑ is the molecular tilt or the angle of the director **n** with respect to the smectic normal $\mathbf{h}||z$ and φ is the azimuthal angle between the **c**-director and a chosen axis, e.g. x. Correspondingly, there are two elastic modes, the soft and Goldstone ones described by changes in ϑ and φ [13]. They are shown in Figure 2. The Goldstone mode is gapless, that is the conical motion of the director has no energy threshold, the director follows the external field in accordance with the sign of the dielectric anisotropy.

The molecular chirality reduces the phase symmetry to C_2 but does not influence the order parameter (1) and the corresponding elastic modes. Due to the layered structure, molecular chirality and the director tilt to the smectic normal, the SmC* phase possesses the structural helicity and local spontaneous polarization. The latter is described by vector $\mathbf{P}_s \perp \mathbf{h}$, **n** with its modulus depending on the tilt angle. At a small tilt, $\mathbf{P}_s$ is just proportional to ϑ. The helical structure shown in Figure 3 is not of the principal importance for our discussion of bistability because, even without an external electric field and limiting surfaces, the helix may be unwound by mixing two *different* compounds of opposite chirality keeping $\mathbf{P}_s$ finite [14]. As shown in Figure 4, there are two "magic points" on the HOBACPC concentration axis: at $c \approx 15\%$ P_s vanishes, at $c \approx 60\%$ the helicity disappears, $q_0 = 2\pi/$

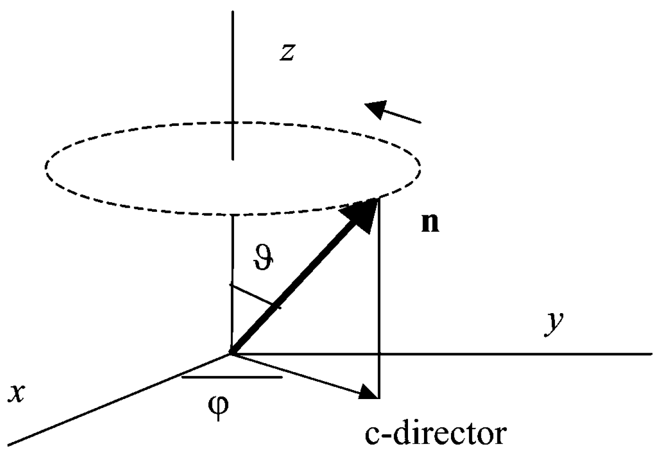

FIGURE 2 Illustration of the conical director motion in the SmC phase.

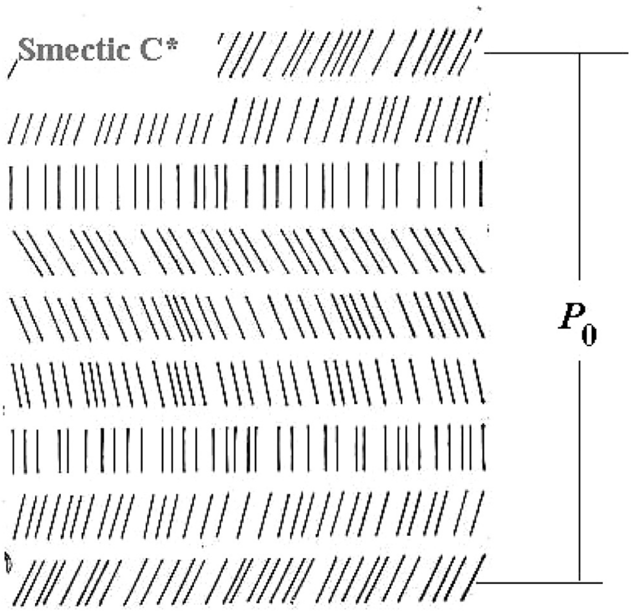

FIGURE 3 Helical structure of the chiral SmC* phase.

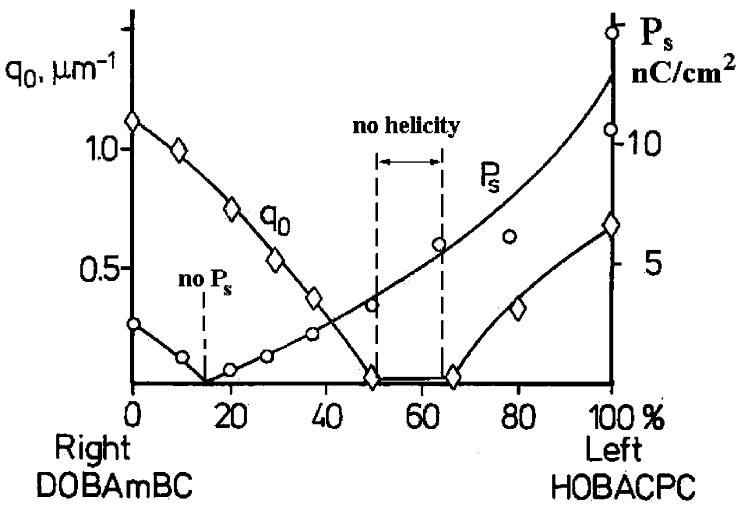

FIGURE 4 The helix wavevector q_0 and the spontaneous polarization P_s as functions of the content of the left-handed HOBACPC in its mixture with right-handed DOBAmBC compound [14].

$P_0 = 0$. Therefore, discarding domain structures, we can design a uniform SmC* phase of infinite volume with finite spontaneous polarization!

In an unlimited stack of smectic layers with fixed **h**, the director is free to rotate along the cone surface being constrained only by condition of $\vartheta = \text{const}$ (Goldstone mode). An external field **E** will interact with $\mathbf{P}_s$ and switch the director without threshold and hysteresis. Therefore the bulk uniform SmC* phase has no that pair of equivalent energy minima which is the principle characteristic feature of a ferroelectric material. Strictly speaking, an unlimited sample of the SmC* phase is not a ferroelectric. It follows the electric field exactly the same way as a magnetic arrow follows the magnetic field. The polar C_2 symmetry corresponds to the class of pyroelectrics. We can imagine that an elongated pyroelectric crystal with plus and minus charges on its ends is suspended in a viscous liquid and, like a rigid electric dipole, is oriented by an electric field in any desirable direction. Therefore our unlimited SmC* phase is nothing more than *a liquid pyroelectric*. It cannot manifest bistability. However, the bistability may appear in thin liquid crystal cells. In this case, the anchoring energy of the director to the substrate plays the key role by stabilising two orientational states with equal energy minima.

3. FERROELECTRIC CELL AND FLC ANCHORING

Here we would like to discuss the simplest conventional description of the FLC cell switching (the so-called Clark-Lagerwall effect [15]) in view of its application to the bistability problem. By a special treatment of limiting glasses one can achieve the so-called bookshelf geometry of an FLC. A convenient presentation of such a surface stabilised (SSFLC) cell is shown in Figure 5 [16]. Here the smectic layers are in the *xy* plane and the easy axis for the director is fixed, for instance, by rubbing both electrodes along *z*. The electric field **E** is applied along the *x*-axis and the director **n** can move along the cone surface with an apex angle of 2ϑ. Its projection on the smectic layer plane (**c**-director) forms an angle φ with respect to the *y*-axis. The spontaneous polarization $\mathbf{P}_s$ is always perpendicular to both **n** and **c** and forms an angle of $\varphi + \pi/2$ with the *y*-axis.

An equilibrium position of the director in SSFLC cells can be described in terms of the **c**-director located between two extreme positions, $\varphi = 0$ and $\varphi = \pi$. Due to the $\mathbf{P}_s$-**E** coupling the electric torque exerted on the director is $P_s E \sin\varphi$ (for simplicity the dielectric anisotropy is neglected). Then the simplified dynamic torque balance

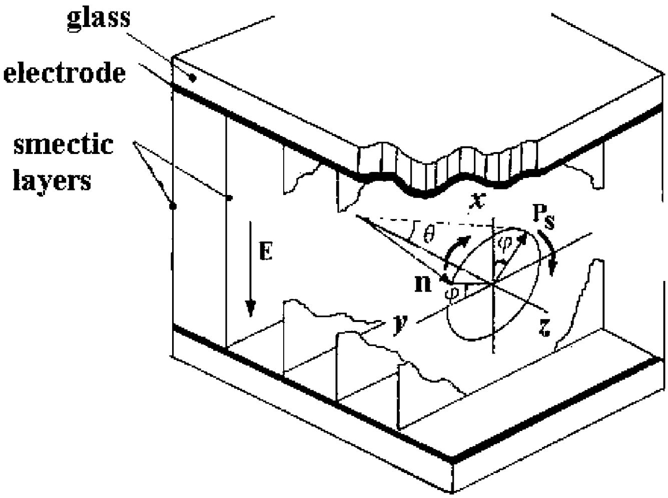

FIGURE 5 Surface-stabilised FLC cell with the bookshelf orientation of smectic layers [16].

equation is written as

$$\xi^2 \frac{\partial^2 \varphi}{\partial x^2} + \sin \varphi = (\gamma_\varphi / P_s E) \frac{\partial \varphi}{\partial t} \tag{2}$$

Here a field coherence length $\xi_C = (K_\varphi / P_s E)^{1/2}$ is introduced and the elastic torque $K_\varphi \partial^2 \varphi / \partial x^2$ is taken in the one-constant approximation with the renormalised "nematic" (K) elastic modulus $K_\varphi = K \sin^2 \vartheta$. On the right side the viscous torque includes the renormalised "nematic" (γ_1) viscosity coefficient $\gamma_\varphi = \gamma_1 \sin^2 \vartheta$.

The boundary conditions generally include the polar (potential V) and quadrupolar (potential W) terms [16,17]:

$$W_s = V \sin \varphi + W \sin^2 \varphi \tag{3}$$

Equation (2) was widely used in literature for the description of the director switching dynamics, but its application to the investigation of the switching threshold and bistability was ambiguous.

Very often the boundary conditions are disregarded at all but the switching is assumed to occur. This corresponds to the condition of the *infinite* elastic modulus K_φ. It seems strange, but namely for $K_\varphi \to \infty$ we may neglect the elastic term due to vanishing derivative $\partial^2 \varphi / \partial x^2$. Then the distribution of the director in the bulk is uniform and the FLC is switched as a "block" , exactly as a pyroelectric crystal suspended in a viscous medium. In this case, the bistability is absent, as discussed above.

In other papers the second term in (3) is disregarded and only the polar term is taken into account. It is assumed that spontaneous polarization $\mathbf{P}_s$ "likes" to be perpendicular to the electrodes due to some polar interaction with the "surface dipoles". In our opinion there is no physical ground for this. Microscopically, molecules of typical smectic C* materials have smaller dipole moments than those of typical nematic materials, but the surface polarization even in nematics is very small [18]. From the macroscopic point of view, the orientation of the $\mathbf{P}_s$ vector perpendicular to the electrodes is unfavorable because it would create its own electric field along the normal to the cell even in the absence of the external field and the free energy would increase. Furthermore, if two electrodes are treated similarly (typical situation) the two $\mathbf{P}_s$ vectors at the boundaries look into the opposite directions and this would create a twist of the director by 2ϑ along the cell normal. Such situation is shown in Figure 6 (left). To have the uniform distribution of the director one should invent special, asymmetric aligning layers orienting the $\mathbf{P}_s$ vectors in the same direction, Figure 6 (right). Had it happened, it would be impossible to have the second equivalent stable state necessary for the bistability. Finally, for majority of FLCs the director is easily oriented along the rubbing

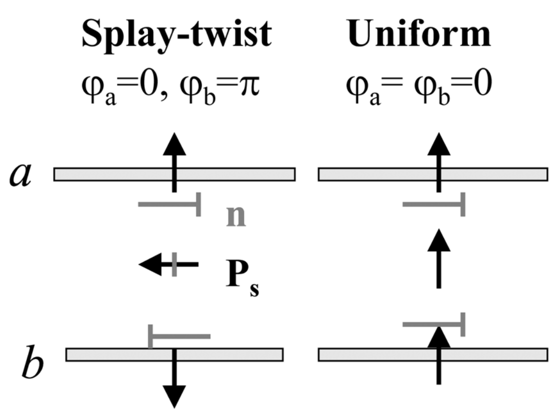

FIGURE 6 Polar anchoring with cylindrical symmetry with respect to the vertical axis. Left: Antiparallel $\mathbf{P}_s$-vectors at the opposite surfaces result in a splayed $\mathbf{P}_s$-structure conjugated with the twisted director structure. The angle between the directors at the opposite surfaces is 2ϑ. Angles of the c-director differ by π. Right: uniform $\mathbf{P}_s$- and $\mathbf{n}$-structure. (See COLOR PLATE I)

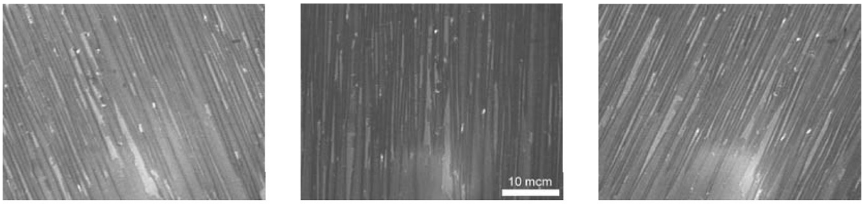

(a) (b) (c)

FIGURE 7 Microscopic photos of the FLC texture oriented by rubbing polyimide layers. The direction of rubbing is vertical. Analyser A is crossed with polariser P. The polariser is at the angle of –24 deg (a), 0 (b) and +24 deg (c) with respect to the rubbing direction (material ZLI-4237-100 from Merck, $\vartheta = 24$ deg, $P_s = 30\,\mathrm{nC/cm^2}$). (See COLOR PLATE II)

direction without the twist. An example is shown in Figure 7, see also [9].

Therefore, we consider the polar anchoring term hardly compatible with bistability and will disregard it further on. Typically the dominating term in the boundary conditions (3) is the quadrupolar one providing two equivalent states for the director ($\varphi \approx \pm\vartheta$ with respect to the rubbing direction) necessary for the bistability and giving the energetically favorable orientation of the $\mathbf{P}_s$ vector, shown in Figure 8. In some papers, the threshold for the switching was discussed using Eq. (2) and the quadrupolar term in (3). Few references can be found in [15] but those results cannot be used for the discussion of bistability phenomena. We believe that the reason lies in the formulation of the boundary conditions in terms of the **c**-director with only one variable φ whereas the director anchoring must be described using two variables. Let consider this problem in more details.

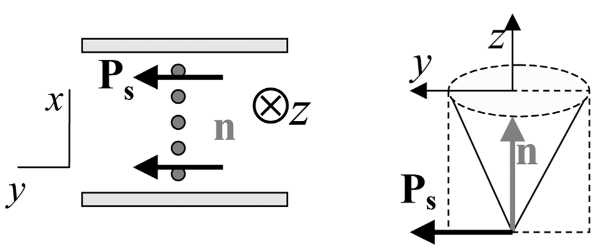

FIGURE 8 Quadrupolar anchoring of the director along the x-direction. Side (left) and top (right) views. (See COLOR PLATE III)

4. ZENITHAL AND AZIMUTHAL DIRECTOR ANCHORING IN SmC*

In our modelling procedure we operate with the director **n** (not with the **c**-director) and consider its anchoring exactly as in the case of nematics. For nematics one introduces two quadrupolar anchoring energies, the zenithal (sometimes called polar, but we avoid this term) and azimuthal ones which can be measured by many different techniques and differ by one or two orders of magnitude [15]. The same consideration can be applied to a SmC*. Here we discuss a simplified approach (for the general case, see [10]).

Consider Figure 9 where the easy axis is directed along z and the director **n** coincides with OA. Then nematic anchoring energies are defined by the zenithal α and azimuthal β angles:

$$W_z = \frac{1}{2} W_z^0 \sin^2\alpha \quad \text{and} \quad W_a = \frac{1}{2} W_a^0 \sin^2\beta \tag{4}$$

Using elementary geometry we can express *the same energies* in terms of ϑ and φ:

$$W_z = \frac{1}{2} W_z^0 \sin^2\vartheta \cdot \sin^2\varphi \quad \text{and}$$

$$W_a = \frac{1}{2} W_a^0 \frac{\sin^2\vartheta \cdot \cos^2\varphi}{1 - \sin^2\vartheta \cdot \sin^2\varphi} \approx \frac{1}{2} W_a^0 \sin^2\vartheta \cdot \cos^2\varphi \tag{5}$$

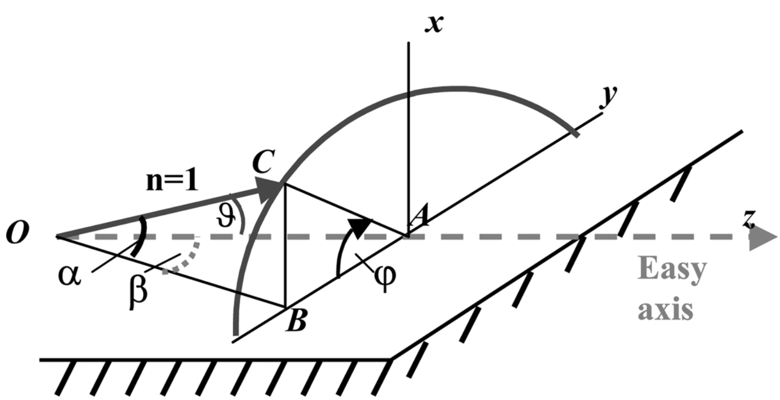

FIGURE 9 Zenithal and azimuthal anchoring for the director (vector **n**) and the **c**-director (represented by angle φ). (See COLOR PLATE IV)

Now, from (5) on account of (3), we can introduce the zenithal and azimuthal anchoring energies for the **c**-director:

$$W_z^{\vartheta} = W_z^0 \sin^2 \vartheta \quad \text{and} \quad W_a^{\vartheta} = W_a^0 \sin^2 \vartheta \tag{6}$$

Note that *the two potentials for the* **c***-director* φ *depend on tilt angle* ϑ *and approximately one order of magnitude less than the corresponding nematic energies*. They are renormalised by factor $\sin^2\vartheta$ exactly the same way as elastic and viscosity coefficients. To our knowledge, this topic has not been discussed in literature. Finally we have two relationships between the nematic and smectic C* anchoring in terms of the φ and ϑ angles:

$$W_z = \frac{1}{2} W_z^{\vartheta} \sin^2 \varphi \quad \text{and} \quad W_a \approx \frac{1}{2} W_a^{\vartheta} \cos^2 \varphi \tag{7}$$

Equation (7) are very important for discussion of the bistability criterion and we come back to them a little later. Now we shall show how the renormalised anchoring energies influence the threshold for the director switching.

5. STATIC THRESHOLD FOR THE DIRECTOR SWITCHING

Experiments show that sometimes the director switching between two stable states has very low threshold (about 1V/μm or less) while in nematics it is typically of about 3–10 V/μm *for the same magnitude of the electric torques* $P_s E$ and $\varepsilon_a E^2$. Now we compare the threshold conditions for the SmC* and a nematic for the infinite and a finite anchoring energy. We are interested in the static threshold, hence, the viscous term in Eq. (2) is disregarded ($\partial\varphi/\partial t = 0$).

a) Infinite Anchoring Energy

At first, consider a planarly oriented nematic with positive dielectric anisotropy ε_a, Figure 10. The field coherence length is

$$\xi_N = \frac{1}{E}\sqrt{\frac{4\pi K}{\varepsilon_a}} \tag{8}$$

At zero field ξ_N is infinite. With increasing field it decreases and becomes comparable with the cell thickness d. The condition $\xi_N = d/\pi$ defines the threshold for the Frederiks transition to the splay-type distortion with a profile shown in the figure:

$$E_F = \frac{\pi}{d}\sqrt{\frac{4\pi K}{\varepsilon_a}} \tag{9}$$

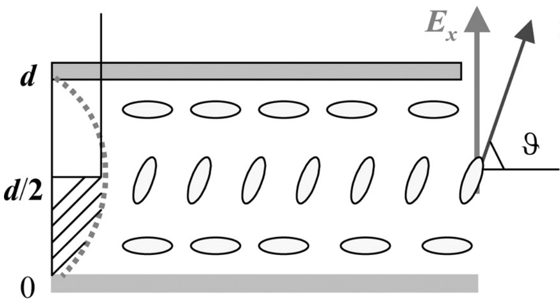

FIGURE 10 Geometry of the splay director distortion slightly above the Frederiks transition in a nematic. (See COLOR PLATE V)

For typical nematics with $K = 10^{-6}$ dyn, $d = 2.5\,\mu\text{m}$, $\varepsilon_a = +10$ we obtain the threshold field $E_F = 14\,\text{statV/cm}$ or $400\,\text{mV}/\mu\text{m}$.

A similar consideration may be applied to the SmC* phase. When the field coherence length ξ_C defined under Eq. (2) becomes comparable with d the twist distortion shown in Figure 11 should appear just above the threshold. Comparing ξ_C from Eq. (2) with cell thickness d we find the Frederiks transition threshold:

$$E_F^* = \frac{\pi^2 K_\varphi}{P_s d^2} \tag{10}$$

For typical values of $K_\varphi = 10^{-7}$ dyn, $d = 2.5\,\mu\text{m}$, $P_s = 100\,\text{nC/cm}^2$ we obtain $E_F^* = 0.05\,\text{statV/cm}$ or $1.5\text{mV}/\mu\text{m}$ (considerably smaller than in nematics). The magnitude of distortion increases with field $E > E_F^*$

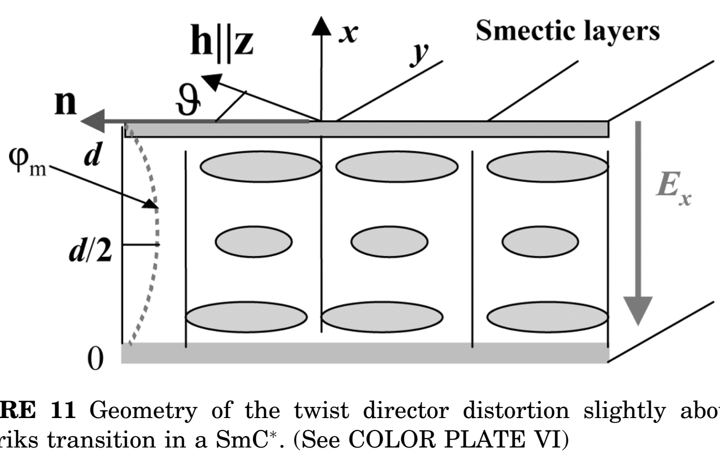

FIGURE 11 Geometry of the twist director distortion slightly above the Frederiks transition in a SmC*. (See COLOR PLATE VI)

but after switching the field off the distortion relax to the initial situation and *no bistability* can be observed for the infinite anchoring.

b) Finite Anchoring Energy

The first effect of the finite anchoring is a slight modification of the Frederiks transition threshold. Now in Eqs. (9,10) instead of cell thickness d we have a sum $d+2b$ where $b=K/W$ is the surface extrapolation length [15]. As a rule $b \ll d$ and a small change in the Frederiks transition threshold is not important for discussion of bistability.

What is of great importance is the so-called "break of anchoring" corresponding to the threshold for the complete tearing the director off from the surface. This effect takes place when the field coherence length becomes comparable with the surface extrapolation length, $\xi_{\mathrm{BA}} \approx b$. Applying this condition to a nematic with $b=K/W_{\mathrm{z}}$ we find the threshold for the break of anchoring:

$$E_{ba}^{N} = \frac{W_z}{K}\sqrt{\frac{4\pi K}{\varepsilon_a}} \tag{11}$$

For $K = 10^{-6}\,\mathrm{dyn}$, $\mathrm{W_z} = 0.3\,\mathrm{erg/cm^2}$, $d = 2.5\,\mu\mathrm{m}$ and $\varepsilon_a = +10$ the threshold field is $E_{ba}^{N} \approx 100\,\mathrm{StatV/cm}$ or $3\,\mathrm{V}/\mu$ (the value typically met in experiments with bistable nematic displays).

For the SmC* phase the break of anchoring corresponds to the threshold for bistability. With $b = K_\varphi / W_z^\vartheta$ we find

$$E_{ba}^{C} = \frac{(W_z^\vartheta)^2}{P_s K_\varphi} \tag{12}$$

With $K_\varphi = 1.2\times10^{-7}$ dyn, $d = 2.5\,\mu$, $P_{\mathrm{s}} = 100\,\mathrm{nC/cm^2}$, $W_{\mathrm{z}} = 0.3\,\mathrm{erg/cm^2}$ (same as for our nematic) and $\vartheta = 20$ deg we shall have $\mathrm{W_z^\vartheta} = 0.036\,\mathrm{erg/cm^2}$ and $E_{\mathrm{ba}}^{\mathrm{C}} = \approx 35\,\mathrm{StatV/cm}$ or $1\,\mathrm{V}/\mu$ (3 times lower than in our nematic). A strict analytical calculation [19] results in the same formula (12) with coefficient $8/27 \approx 0.3$, further reducing the threshold.

More general, due to the quadratic dependence of the threshold (12) on the anchoring energy, when the "nematic energy" $\mathrm{W_z} < 1\,\mathrm{erg/cm^2}$, *the threshold for the break of anchoring in SmC* is lower than in typical nematics*. For $\mathrm{W_z} < 0.1\,\mathrm{erg/cm^2}$ the difference will be dramatic even for smaller P_{s}. This explains the low threshold for the bistability of SmC* materials with $P_{\mathrm{s}} \approx 20$–$30\,\mathrm{nC/cm^2}$.

There is one more factor, which further facilitates the break of anchoring in SmC*. Actually the presence of the polarization in the case of the director deformation would results in an inhomogeneous electric field distribution along the cell normal. Above the Frederiks transition, a form of the distortion depicted in Figure 11 is no longer accurate. The arising inhomogeneity in the electric field distribution stabilises the homogeneous director distribution across the whole thickness. Now it looks like an elongated trapezoid instead of the half-period sine form. Thus the director deformation becomes basically located close to the surfaces with the field strength increased there. However, this is not the whole story and in the next Section we shall see how the static threshold for the bistable switching of a SmC* may even be reduced to zero.

It should be noted that the static threshold discussed cannot be found from the measurements of the width w of the hysteresis loop, which is usually observed with the alternating external voltage of the sine or triangular form. In this, dynamic regime the coercive field equal to $w/2$ originates from the right-side term in Eq. (2). It depends on the FLC viscosity γ_φ [20], which determines the phase lag between the external field and the director orientation.

6. THE CRITERION FOR BISTABILITY RELATED SOLELY TO ANCHORING

Let come back to Eq. (7) and assume for a moment that the zenithal and azimuthal anchoring energies are equal. Then the sum of them becomes independent of φ:

$$W^\vartheta \approx W^0 \sin^2 \vartheta(\sin^2 \varphi + \cos^2 \varphi) = W^0 \sin^2 \vartheta \tag{13}$$

What does it mean? It can easily be understood from Figure 5. When $\varphi = 0$, the director is at the surface of an electrode, the zenithal energy is zero, but azimuthal one is maximum and tries to return the director to its initial position with $\varphi = \pi/2$ defined by the rubbing procedure. However, when $\varphi = \pi/2$ the zenithal energy is maximum and tries to return the director back to the state with $\varphi = 0$. The two energies compete with each other and the director does not feel the boundaries. Therefore, a condition

$$W_z^0 = W_a^0$$

means that there is neither a threshold for the director motion along the cone, nor characteristic stable states. Hence, there is neither switching hysteresis nor bistability.

It is evident that to have the true bistability the zenithal energy must exceed the azimuthal one. The principal and necessary criterion for the bistability is a *finite positive energy difference*:

$$W_{za} = W_z - W_a > 0 \tag{14}$$

Clearly this result could not be found from the simplest consideration based on the boundary conditions in the form of Eq. (3). It follows also from our modelling. We have fixed the zenithal anchoring energy at the value of $W_z = 1\,mJ/m^2$ (i.e. $1\,erg/cm^2$) and varied the value of the azimuthal energy W_a. The electric field form shown at the bottom of Figure 12 is suitable for the analysis of the director switching by the optical transmission of an FLC cell placed between crossed polarizers with the front polariser at an angle of 24deg with respect to the rubbing direction. All relevant parameters are presented in the caption to the figure. As will be discussed in the next section, the insulating alignment layers of finite thickness d_p can dramatically influence the optical response. To avoid these complications here, the specific

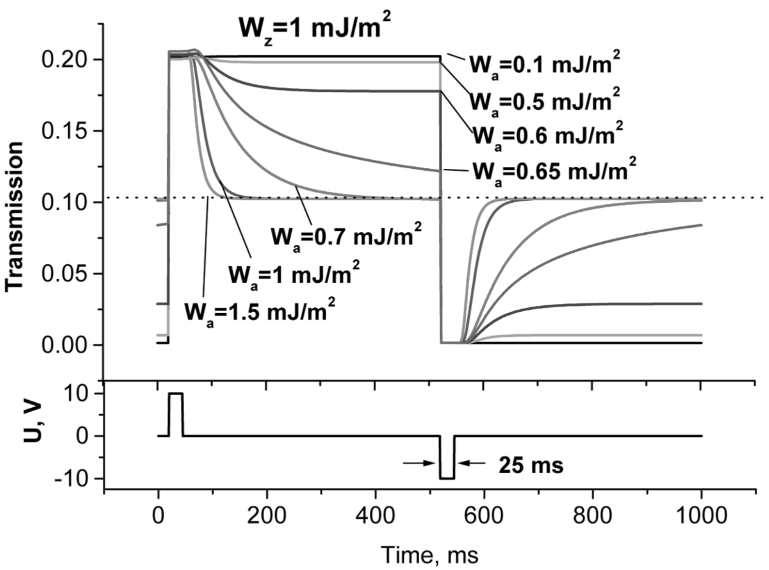

FIGURE 12 Optical transmission showing the relaxation of the field induced states upon variation of the azimuthal anchoring energy W_a for the zenithal energy fixed at $W_z = 1\,mJ/m^2$. Other model parameters are: Material: ZLI 4237-100 ($P_s = -20\,nC/cm^2$, $\varepsilon_{||} = 3$, $\varepsilon_{\perp} = 4.2$, $\rho_{lc} = 10^8\ \Omega m$, $n_{||} = 1.67$, $n_{\perp} = 1.53$, $\vartheta = 24$deg, Frank moduli $K_{1,2,3} = 10\,pN$, compressibility modulus $K_4 = 5\,MPa$, $\gamma_{\varphi} = 0.18$ Pa.s, helical pitch $h = 10\,\mu m$; Cell parameters: bookshelf structure, area $4 \times 4\,mm$ $d_{lc} = 2\,\mu m$, $d_p = 40\,nm$, $\rho_p = 6.10^7\ \Omega m$ ($G_p = 3.3\,\mu S$), $\varepsilon_p = 5$, pretilt angle $\vartheta_s = 5$deg. (See COLOR PLATE VII)

resistance of the alignment layers was chosen to be very low, $\rho_p = 6.10^7$ Ωm (the layers are extremely conductive).

From Figure 12 it is seen that for W_a less than about half of W_z the optical response is bistable, at least over the range of a second. When W_a approaches the W_z value, the relaxation time of the two field induced states becomes shorter and, for $W_a = W_z$, reaches the value of 50ms and continues to shorten for $W_a > W_z$. We conclude that for W_a close to W_z *the bistability vanishes even in the case of strongly conductive alignment layers*.

Therefore, we have confirmed the static bistability criterion (14). This criterion (the necessary condition) controls the bistability in the absence of insulating alignment layers or in the case of very conductive alignment layers. In the opposite case, we need the additional (and sufficient) condition for the bistability related to a new factor, the internal electric field discussed below.

7. ALIGNMENT LAYERS AND BISTABILITY

The role of alignment layers in the bistability phenomena has been widely discussed in literature. Here we shall formulate a new criterion governing the bistable or monostable switching and taking into account the dielectric and conductive properties of both the liquid crystal and alignment layers. However, to make the physics of the phenomenon more transparent we begin with a consideration of the pure electrostatic case.

a) Non-conductive FLC and Alignment Layers

A bilayer system between two electrodes is shown in Figure 13. The thicker layer mimics a non-conductive FLC layer with the polarization

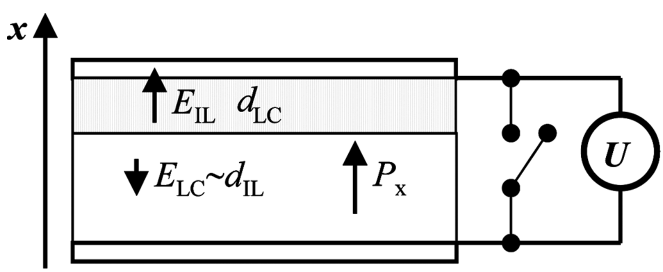

FIGURE 13 Insulating FLC and alignment layers. The arrows show the directions of the internal fields in both layers at $U = 0$.

P_x – component directed up. The thinner layer mimics two insulating alignment layers with their capacities connected in series. The equations for continuity of displacement D_x and for distribution of voltages over the contour read:

$$\begin{aligned} \varepsilon_{IL}E_{IL} &= \varepsilon_{LC}E_{LC} + 4\pi P_x \equiv D_x \\ d_{IL}E_{IL} + d_{LC}E_{LC} &= U \end{aligned} \tag{15}$$

From here we can easily find the electric field in the two layers:

$$E_{LC} = \frac{\varepsilon_{IL}U - 4\pi P_x d_{IL}}{(\varepsilon_{LC}d_{IL} + \varepsilon_{IL}d_{LC})} \quad \text{and} \quad E_{IL} = \frac{\varepsilon_{LC}U + 4\pi P_x d_{LC}}{(\varepsilon_{LC}d_{IL} + \varepsilon_{IL}d_{LC})} \tag{16}$$

Due to the presence of polarization the electric field exists in each layer even at $U = 0$ and the two fields are opposite to each other, as shown in Figure 13. *At $U = 0$ the internal field in the liquid crystal layer is always opposite to P_s*. Due to this, the electrostatic threshold for the bistability should exceed the threshold for the break of anchoring of the FLC by the modulus of this field:

$$E_{BS}^{elst} = E_{ba}^{*} + \left| \frac{P_x d_{IL}}{\varepsilon_0(\varepsilon_{LC}d_{IL} + \varepsilon_{IL}d_{LC})} \right| \tag{17}$$

For typical parameters $d_{IL} = 2 \times 0.04\,\mu\text{m}$, $d_{\text{LC}} = 2\,\mu\text{m}$, $\varepsilon_{IL} = 5$, $\varepsilon_{\text{LC}} = 3$, $P_x = 100\,\text{nC/cm}^2$ the magnitude of this additional field is about $0.6\,\text{V}/\mu\text{m}$. Therefore, for FLC with high P_s the internal field can be comparable with the field necessary for the break of anchoring. It is not favorable for the bistability.

b) Conductive FLC and Alignment Layers

In this, more realistic, dynamic case the analysis is more difficult. The qualitative picture based on an assumption that FLC has field independent dielectric constant ε_{LC} has been considered in Ref. [9]. Here it is sufficient to underline an importance of the following inequality:

$$\tau_{\text{LC}} = \varepsilon_{\text{LC}}\rho_{\text{LC}} \geq \varepsilon_{\text{p}}\rho_{\text{p}} = \tau_{\text{p}} \tag{18}$$

Here τ_{LC} and τ_{p} are Maxwell space charge relaxation times for the FLC and alignment polymer layers, respectively.

According to criterion (18), due to the existence of the internal field in the FLC layer, -non-conductive FLC combined with fairy conductive alignment layers promote True Bistability -conductive FLC combined with insulating alignment layers suppress bistability and even promote Inverse Bistability [9].

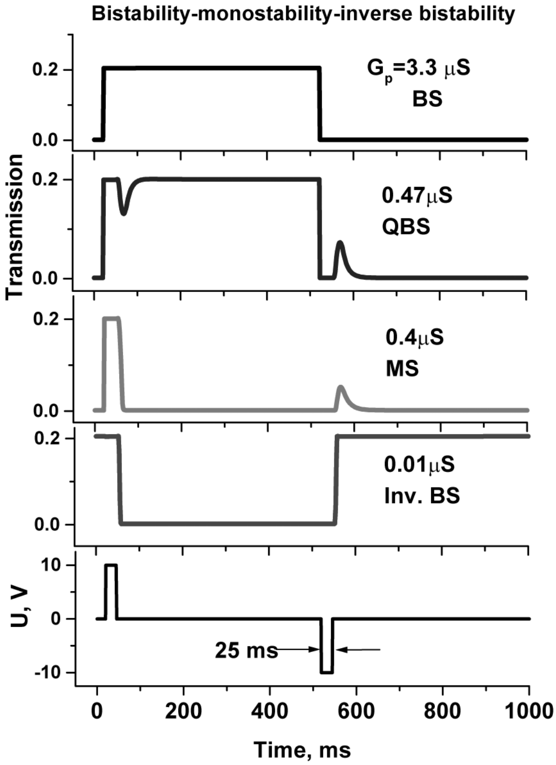

FIGURE 14 From the top to the bottom: kinetics of the optical transmission showing true bistability (BS), quasi bistability (QBS), monostability (MS) and inverse bistability (IBS) upon variation of conductivity of alignment layers. $W_z = 1\,mJ/m^2$, $W_a = 0.1\,mJ/m^2$, $\rho_{lc} = 10^8\ \Omega m$, for other parameters see the caption to Figure 12.

The modelling (without assumption of $\varepsilon_{LC} = const$) has confirmed criterion (18). The result is shown in Figure 14, which presents the effect of the alignment layer conductivity on bistability. The form of the applied voltage is the same as in Figure 12. The main criterion (14) is fulfilled from the beginning: $W_z = 1\,mJ/m^2 > W_a = 0.1\,mJ/m^2$ and the conductivity of the FLC layer is fixed at $\rho_{lc} = 10^8\ \Omega m$ (cell conductivity $G_{LC} = 0.08\,\mu S$). The alignment layer conductivity decreases from $3.3\,\mu S$ to $0.01\,\mu S$ upon proceeding from the top to the bottom and the transmission curves manifest different regimes of switching.

(i) In the range of G_p from infinity to about $1\,\mu S$ the *true bistability* (BS) is observed as we have seen in Figure 12. In this regime the director is driven by the positive electric pulse E_{ext} from, say, its "left" into its "right" stable state and the internal field is negligible.

(ii) With decreasing G_p a spike appears just at the end of the driving pulse (the curve for $G_p = 0.47\,\mu S$). This spike is due to an opposite internal field E_{int} that is still weak and acting for a short time. It can partially deviate director from the final "right" stable state but not sufficient to break its new anchoring. We can call this regime *quasi-bistable* (QBS).

(iii) Further decrease in G_p (curve for $G_p = 0.4\,\mu S$) results in the *monostable* regime (MS) experimentally observed in [11]. Now the director is driven by positive E_{ext} close to the "right" stable state but negative E_{int} is quite strong and competing with E_{ext}. Its time dependence is shown in Figure 15. Due to the influence of E_{int} the director returns to its initial "left" position and the next, this time negative E_{ext} pulse cannot switch the director. Only new internal field of the positive sign slightly deviates the director from the initial state but is not high enough to break anchoring.

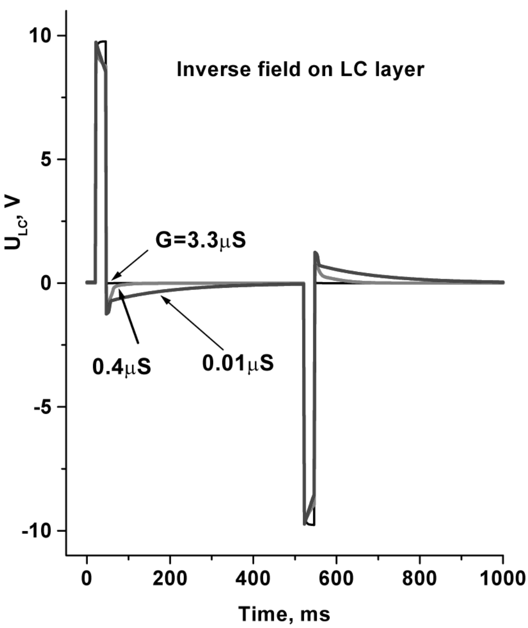

FIGURE 15 Kinetics of the internal field in the FLC layer upon variation of conductivity of alignment layers. All parameters correspond to Figure 14. (See COLOR PLATE VIII)

(iv) Finally, for the lowest conductivity $G_p = 0.01\,\mu S$ (or for completely insulating layers) the inverse internal field becomes high enough to overcome the effect of the field of preceding driving pulses and results in what we call "*an inverse bistability*" (IBS): positive external voltage tends to drive the director to the "right" position but the following negative "tail" of the internal field (see Fig. 15) sticks the director to the left stable position. Then the process repeats. It is interesting that the inverse bistability has been observed in drops of FLC embedded into an insulating polymer matrix [12]. Recently the same effect has been found in the Institute of Crystallography (Moscow) in conventional FLC cells with the bookshelf geometry and thick (about 100 nm) insulating alignment layers [9,21].

8. ALIGNMENT LAYERS AND THE ELECTROOPTICAL V-SHAPE EFFECT

When a triangular voltage form is applied to the SSFLC cell one can observe hysteresis of polarization. When the polarization is switched up and down by voltage U, the director is switched left and right through the angle close to the director tilt angle $\pm\vartheta$. In this case the polarizer is parallel to the rubbing direction, the analyser is in the crossed position and the optical transmission curves are symmetric with respect to the line $U = 0$. Usually the director is also switched with a hysteresis and the optical transmission has the form of letter "W". The distance between the bottom apices of this letter is equal to the double coercive field related to both the viscous phase lag mentioned at the end of Section 5 and the threshold for the bistable switching.

However, when the period of the external field is fixed typically within a range of 1–10 Hz and insulating or weakly conductive alignment layers become thicker and thicker, the coercive field decreases. Then two apices of the "W" letter approach each other and then coincide at the zero external voltage. The same result could be achieved if we fix all parameters of the FLC cell and vary frequency of the applied triangular field. At a certain frequency the switching becomes hysteresis-free and the electrooptical response acquires a form of the "V" letter shown in Figure 16. For the first time, this effect was observed by the Fukuda group [22] (see also [3]). It is very interesting for applications to the display technology due to feasibility of multiple grey scale levels.

Our experiments and modelling show [5–8,10] that the hysteresis free switching is controlled by the internal field in a FLC, which in turn comes from dividing the external voltage between the FLC and

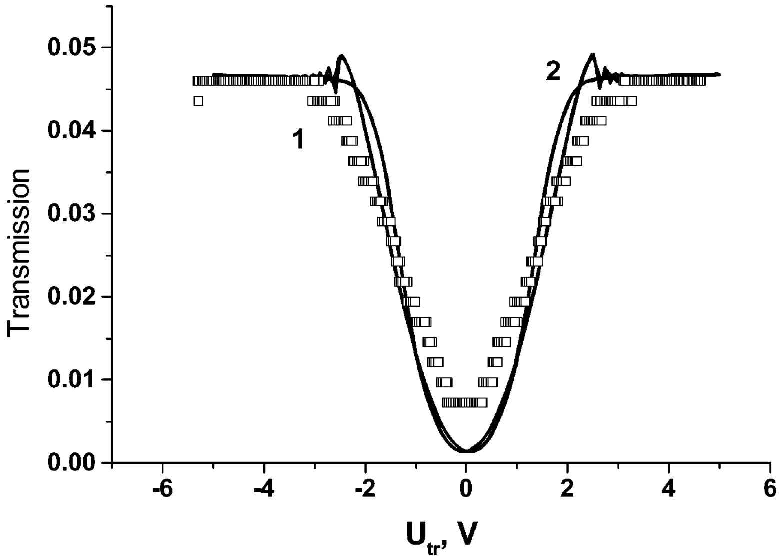

FIGURE 16 Experimental (1) and calculated (2) oscillograms of the optical transmission of 0.85 μm thick cell filled with Zk-438 (NIOPIK, $P_s = 85\,\mathrm{nC/cm^2}$) as functions of triangular voltage ±10V, frequency 95 Hz. Other parameters are specified in Ref. [8].

two alignment layers. Surely, the field in the FLC changes its form and magnitude due to a different phase shift of different harmonics of the triangular voltage form. Moreover, small capacitance C_p of thick insulating layers being connected in series with the FLC layer stabilises the magnitude of the current in FLC, because the latter, due to switching of high P_s, has very large dynamic dielectric permittivity. With triangular voltage pulses the current $C_p dU/dt$ becomes nearly constant (positive or negative within each half-period) and the field on the FLC layer tends to zero [10]. Over a certain frequency the phase lag between the external field and the director disappear and the large "dynamic" part of the coercive field related to viscosity vanishes. The hysteresis loop becomes very narrow as if the cell were in the static regime! When the static thresholds discussed in Section 5 are absent or very low we have the ideal hysteresis-free switching (genuine V-shape regime). When they are not as low, the electrooptical response is *practically* close to the V-letter.

In fact, the phenomenon of the hysteresis free switching is opposite to the bistability and what is good for bistability is bad for the V-shape effect. It is the other side of the same coin. For example, the hysteresis-free switching is promoted by thick, weakly conductive layers, enhanced spontaneous polarization, enhanced conductivity of an FLC and proximity of the two anchoring energies W_a and W_z.

9. CONCLUSION

We have developed a new approach to the anchoring of the director and a new modelling procedure operating with the director **n** (not φ). In our new treatment of the bistability, we take a proper account of both azimuthal W_a and zenithal W_z energies of the SmC* phase. If we compare these energies with corresponding "nematic" ones we can see that, due to the factor of $\sin^2\vartheta \approx 0.1$, the "apparent" SmC* energies W_a and W_z are about 10-times smaller than their nematic counterparts! This is the reason why the threshold field for the anchoring break that is the threshold for the SmC* switching is very low. Our numerical calculations show that the interplay between W_a and W_z is crucial for the bistability. For example, when $W_a = W_z$, the field-induced conical motion of the director becomes thresholdless even in surface stabilized cells (no bistability). The bistability is possible when inequality (14) has been fulfilled.

The second important factor determining the threshold for switching and other properties of ferroelectric cells is finite impedance of the alignment layers. In fact, new criteria for the bistability (18) have been found for the cells with conducting alignment layers. Varying solely parameters of these layers (thickness, dielectric constant and resistance) we can smoothly change a switching regime from strongly bistable to hysteresis-free. Varying additionally liquid crystal parameters and the two anchoring energies we can fit the performance of ferroelectric cells to many particular applications.

REFERENCES

[1] Meyer, R. B., Liebert, L., Strzelecki, L., & Keller, P. (1975). *J. Physique (Lett)*, *36*, L69.
[2] Clark, N. A. & Lagerwall, S. T. (1980). *Appl. Phys. Lett.*, *36*, 899.
[3] Lagerwall, S. T. (1999). "*Ferroelectric and antiferroelectric liquid crystals*", Wiley-VCH: Weinheim, 390.
[4] Yang, K. H., Chieu, T. C., & Osofsky, S. (1989). *Appl. Phys. Lett.*, *55*, 125.
[5] Blinov, L. M., Pozhidaev, E. P., Podgornov, F. V., Pikin, S. A., Palto, S. P., Sinha, A., Yasuda, A., Hashimoto, S., & Haase, W. (2002). *Phys. Rev. E*, *66*, 021701.
[6] Blinov, L. M., Palto, S. P., Podgornov, F. V., Moritake, H., & Haase, W. (2004). *Liq. Cryst.*, *31*, 61.
[7] Palto, S. P., Blinov, L. M., Podgornov, F. V., & Haase, W. (2004). *Mol. Cryst. Liq. Cryst.*, *410*, 95.
[8] Blinov, L. M., Palto, S. P., Andreev, A. L., Pozhidaev, E. P., Podgornov, F. V., & Haase, W. (2004). *Mol. Cryst. Liq. Cryst.*, *410*, 105.

[9] Palto, S. P., Geivandov, A. R., Barnik, M. I., Blinov, L. M. On a role of alignment layers in bistable switching of ferroelectric liquid crystals. *Numerical simulations and experimental results*. Ferroelectrics (in press).
[10] Palto, S. (2003). *Crystallography Reports*, *48*, 24.
[11] Vorflusev, V., Kosygina, M., & Chigrinov, V. (1996). *Ferroelectrics*, *178*, 75.
[12] Pozhidaev, E. & Haase, W. (2003). In: *"Relaxation Phenomena (Liquid Crystals, Magnetic Systems, Polymers, High-Tc Superconductors, Metallic Glasses)"*, Haase, W. & Wrobel, S. (Eds.), Springer-Verlag: Berlin-Heildelberg, Sect. 5.6, 376–99.
[13] Muševič, I., Blinc, R., & Žekš, B. (2000). *"The physics of ferroelectric and antiferroelectric liquid crystals"*, World Scientific: Singapore.
[14] Beresnev, L. A., Baikalov, V. A., Blinov, L. M., Pozhidayev, E. P., & Purvanetskas, G. V. (1981). *JETP Lett.*, *33*, 536.
[15] Blinov, L. M. & Chigrinov, V. G. (1994). *"Electrooptic effects in liquid crystal materials"*, Springer: New York.
[16] Handschy, M. A. & Clark, N. (1984). *Ferroelectrics*, *59*, 69.
[17] Pikin, S. A. (2003). In: *"Relaxation Phenomena (Liquid Crystals, Magnetic Systems, Polymers, High-Tc Superconductors, Metallic Glasses)"*, Haase, W. & Wrobel, S. (Eds.), Springer-Verlag: Berlin-Heildelberg, Sect. 5.2, 274–309.
[18] Blinov, L. M., Barnik, M. I., Ohoka, H., Ozaki, M., Shtykov, N. M., & Yoshino, K. (2001). *Eur. Phys. J. E*, *4*, 183.
[19] Schiller, P. (1986). *Cryst. Res. Tech.*, *21*, 167.
[20] Reynaerts, C. & de Vos, A. (1991). *Ferroelectrics*, *113*, 449.
[21] Barnik, M. I. & Geivandov, A. R. (unpublished results).
[22] Inui, S., Iimura, N., Suzuki, T., Iwane, H., Miyachi, K., Takanishi, Y., & Fukuda, A. (1996). *J. Mater. Chem.*, *6*, 671.